Characterization of Infrared Range-Finder PBS-03JN for 2-D Mapping[*]

Majd Alwan, Matthew B Wagner, Glenn Wasson, and Pradip Sheth

Medical Automation Research Center	*School of Mechanical Engineering*	*Computer Science Department*	*Department of Mechanical & Aerospace Engineering*
University of Virginia	*Purdue University*	*University of Virginia*	*University of Virginia*
Charlottesville, VA, US	*West Lafayette, IN, US*	*Charlottesville, VA, US*	*Charlottesville, VA, US*
ma5x@virginia.edu	*mwagner@purdue.edu*	*wasson@virginia.edu*	*Pns7q@virginia.edu*

Abstract - **This paper presents a characterization study of the HOKUYO PBS-03JN Infrared range-finder and compares it to the characterization of the SICK LMS-200 laser range-finder for use in indoor 2-D mapping. Many parameters that could affect the performance of the sensor including warm-up time, divergence of the detection beam, usable detection range in the azimuth, target surface, color, and size properties, incidence angle at the target, and the mixed pixels problem have been studied. This characterization, quantification of errors, and 3-D confidence in the distance readings of the sensor is vital for practical applications. These characteristics are compared to the counterpart characteristics of the laser range-finder. The PBS-03JN is a cost effective alternative to laser range-finders in indoor environments. The sensor is attractive due to lower power consumption, and its lightweight.**

Index Terms - Infrared Range-Finders, Distance Measurement Errors, Target Color, Target Surface, Incidence Angle.

I. INTRODUCTION

Obstacle detection is essential to the development of 2-D and 3-D dynamic environmental models for autonomous mobile robots, autonomous guided vehicle, as well as similar user-propelled systems. The pursuit of appropriate sensor technologies has been riddled with issues including cost, accuracy, susceptibility to interference and noise. Many different sensor technologies have been used to develop 2-D environmental models including ultrasonic, laser, and infrared range-finders. Ultrasonic sensors are popular due to their low cost, small size, low power consumption, and relatively simple signal processing requirements, which facilitate operation in real-time [1]. However, ultrasonic range finders have several drawbacks including low angular resolution, slow data collection rate about the azimuth (due to longer time-of- flight), specular reflection, sensitivity to changes in temperature and humidity, and relatively low accuracy in distance measurements compared to their laser counterparts. In addition, their annoying clicking sound when operating makes them less attractive for practical applications that involve a human user. In addition to the uncertainty in distance measurement, the ultrasonic transducer's wide beam angle (30° for the popular Polaroid Ultrasonic range finders [2]) results in greater uncertainty in the width of detected obstacles and/or the true location of the obstacle relative to the center of the detection cone [1, 3]. Multiple sensors are therefore used where the detection cones of contiguous sensors overlap. Additionally, probabilistic and possibilistic fusion functions, such as those reviewed and discussed in [4], are employed to reduce the angular uncertainties of the distance measurements. 2-D laser scanners, on the other hand, have been widely used and studied for applications including object following and obstacle avoidance feature extraction, map building, and self-localization [5]. Laser range-finders provide more accurate range data over a longer detection range with higher angular resolution but are more expensive, bulkier, and heavier than ultrasonic and infrared sensors [1, 6, 7]. There is a need for a cost-effective sensor that can be used in 2-D mapping for mobile robotics. Recent advances in technology have made the use of infrared sensors for 2-D map building possible and attractive due to their lower cost than comparable sensors capable of providing similar distance and directional information [8]. The infrared range finder may be the best alternative to ultrasonic and laser range-finders and thus needs to be characterized and further evaluated for these purposes.

In this paper we characterize the PBS-03JN infrared range-finder in a fashion similar to that employed by Ye and Borenstein to characterize the SICK LMS-200 laser scanner in [5]; a comparison between the two range finders is then made. The remainder of the paper is organized as follows: section II provides an overview of the manufacturer's technical specification; section III describes the experimental setup used to characterize the infrared range-finder and the results are presented in section IV. The paper concludes with a detailed comparison of the PBS-03JN sensor and the laser scanner SICK LMS 200. This comparison is important because, as of this writing, the PBS-03JN is approximately 1/4th the cost of a laser scanner.

II. CHARACTERISTICS OF THE INFRARED SENSOR PBS-03JN

The PBS-03JN infrared sensor, manufactured by HOKUYO AUTOMATIC CO., LTD, contains a mechanically rotating LED that transmit light at a wavelength of 880nm and scans the semi-circular area in front of the sensor at 1 rev./100msec measuring time-of-flight. The sensor takes 121 distance measurements across a 217.8° arc, the 11 measurements on the extreme left and right are not within the sensors "guaranteed" detection zone.

Hence, the usable scan then covers a 178.2° arc giving the sensor an angular resolution of 1.8°. The output response time is 180ms or less (for the sensor's digital outputs when an obstacle is detected inside a pre-defined "protected region"). The sensor's measurement origin is the center of the axial rotation, 3.1 cm from the front of the sensor. The data transfer rate is fixed at 57.6 kbps. The sensor is small, 75 x 70 x 60 mm, and weighs only 500 g. This sensor is intended for indoor use since sunlight may cause erroneous measurements [9] (as is the case with the LMS 200 Sick Laser Scanner [10]). Table I summarizes the manufacturer's specifications of the PBS-03JN sensor [6].

TABLE I
PUBLISHED SPECIFICATIONS OF PBS-03JN INFRARED RANGE-FINDER

Items	Specifications
Size	75x70x60mm
Total Weight	500g
Resolution of Direction Angle	1.8°
Scanning Range	217.8°
Range of distance	20-300cm
Interface Method	RS-232C
Response Time	180msec or less
Power Source	24VDC
Origin of Sensor Range Detection	Axis of rotation (3.1cm from the front of the sensor)

Figure 1 shows the scan process of the PBS-03JN sensor, as well as its guaranteed detection range as specified by the manufacturer.
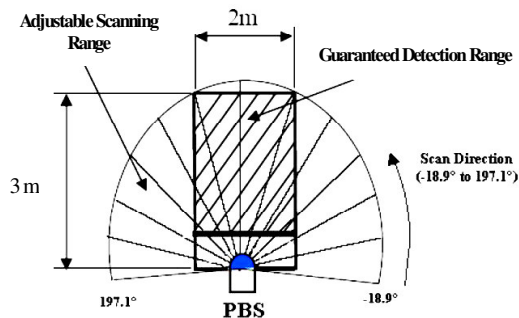

Fig. 1. Scan Process and Guaranteed Detection Range: The sensor scans from –18.9° to 197.1° with a guaranteed range 2m wide and from 0.2m to 3m from the sensor's origin.

III. EXPERIMENTAL SETUP

The experimental setup for the characterization of the accuracy of the PBS-03JN infrared sensor is depicted in Figure 2. The sensor was mounted 0.2m above ground, with its base parallel to the ground, on a 4.5m level track. Targets were then slid along this track to specified distances for each test. The sensor was realigned before each test using levels to ensure the scanning plane remained parallel to the ground and that the center of the sensor was aligned with the track. The alignment was then confirmed by using the PBS configuration software to make small adjustments, by rotating the sensor slightly until the "center" beam at 89.1° returned a distance reading that was closest to the actual target distance. To measure the divergence of the scanning beam, the sensor was rotated 90 degrees so that the top of the sensor was perpendicular to the ground and could be moved to set distances along the X-axis on the 4.5m track. A target was moved across a perpendicular plane until it could be detected by the center beam. This setup is shown in Figure 3.
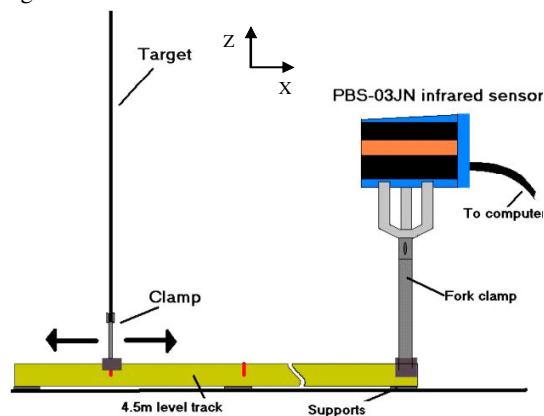

Fig. 2. Experimental Setup #1: The sensor is mounted 20 cm above the ground on the track with the target centered in front of the sensor's origin.
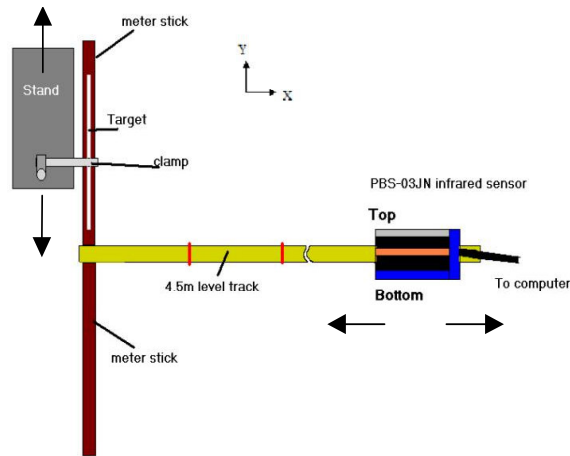

Fig. 3. Experimental Setup#2 for Measuring Beam Divergence in the Elevation plane: The sensor is mounted so that the beam at 89.1° reads along the track. The target is moved along the Y-axis meter stick until it comes into the sensor's view; the sensor can be moved along the X-axis, on the 4.5m track.

All tests were performed indoors with overhead fluorescent lighting at a temperature of approx. 73°F. The sensor was powered from a 24VDC-power supply and was connected to the serial port of a Windows 98 computer running the PBS Configurator software Version 1.1.0, by Hokuyo Automatic Co., LTD. All other tests we performed with the target perpendicular to the sensor's scanning beam unless otherwise specified. Standard Deviation, % error, and % confidence are calculated using the following equations:

$StDevP = \sqrt{\dfrac{n\sum x^2 - \left(\sum x\right)^2}{n^2}}$ (1), where x is the sensor's distance measurement and n is the number of samples.

$\%Error = \left|\dfrac{x - X}{X}\right| * 100$ (2), where x is the measured distance and X is the actual target distance. $\%Confidence = 100 - \%Error$ (3).

VI. CHARACTERIZATION RESULTS

This section presents the experimental results and analysis of the characterization results of the infrared range-finder. The tests include the effect of warming-up (i.e. thermal drift), the divergence of the scanning beam, the effect of target position, size and surface properties on usable detection range, incidence angle at the target, and the "mixed pixels" problem. All distance data were measured along an azimuth of 89.1° (the scan azimuth closest to 90°) with 300mm x 300mm targets unless otherwise specified.

A. Thermal Drift

An RGB 127 target[†] was placed 2.031m from the origin of the sensor and 40,000 data samples were acquired in four consecutive sets of 10,000 samples each with 40 seconds between each set. The data was acquired in four separate sets as the sensor's Configurator software could capture a maximum of 10,000 samples per test. Figure 4 shows the trend of in the raw measurements and the effect of thermal drift over 68.66 minutes, starting with the sensor at room temperature. The sensor required 77.8 minutes for the mean of the measurements to reach a steady state.
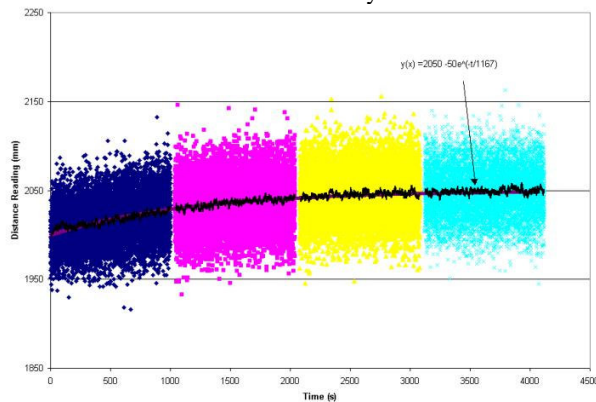

Fig. 4. Thermal Drift: Data fluctuates around the mean, which follows a first order step response and converges to a reading of 2050mm.

The thermal drift response is that of a first order system with a time constant τ=1167 sec.; the thermal drift of the mean of the measurements can be represented by the following exponential equation: $y = 2050 - 50 * e^{t/1167}$ .... (4).
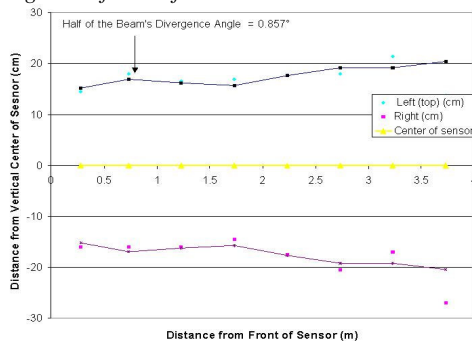
B. Divergence of the Infrared Beam

Fig 5. Beam Divergence in the Elevation plane: The vertical distance from the track at which the target was detected versus the target's horizontal distance from the center of the sensor.

[†] The target is a uniform grey square produced by a laser printer. Each of the R, G and B values of the square's color are set to 127.

The Experimental Setup shown in Figure 3 was used to determine the divergence of the infrared detection beam, measured in the elevation plane. The sensor was moved between 281mm and 3731mm from an RGB 127 target, in increments of 500mm. The target was moved into the sensor's detection cone from the top and bottom of the sensor (see figure 3) until a stable reading was obtained. Figure 5 shows the vertical distance from the track at which the target was detected versus the target's distance from the center of the sensor (i.e. between the emitter and detector). The infrared beam's divergence is computed and found to be approximately 2*0.857°= 1.714°.

C. Measurement Errors with Target Distance and Azimuth

The experimental setup#1, depicted in figure 2, was used in this characterization. The sensor was rotated about the Z-axis, from 0° to 180° in 10° increments. At each angle the RGB 127 target was moved from 221mm to 4221mm in 0.5m increments. An additional test at 3031mm was performed because this distance is on the border of the maximum guaranteed detection area. Figure 6 shows the raw distance measurements about the azimuth, together with the actual target distances; the plot clearly justifies the guaranteed detection region specified as 3m x 2m by the manufacturer.
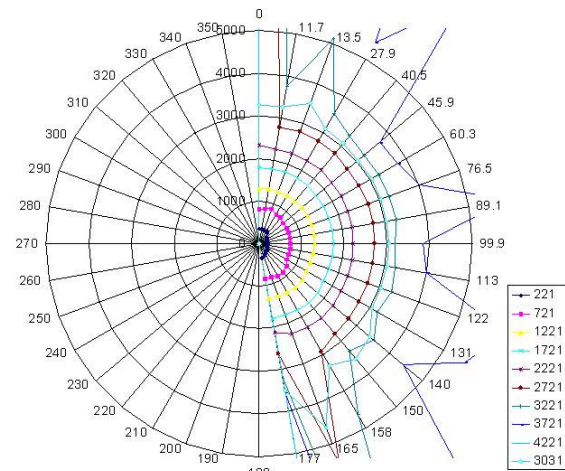

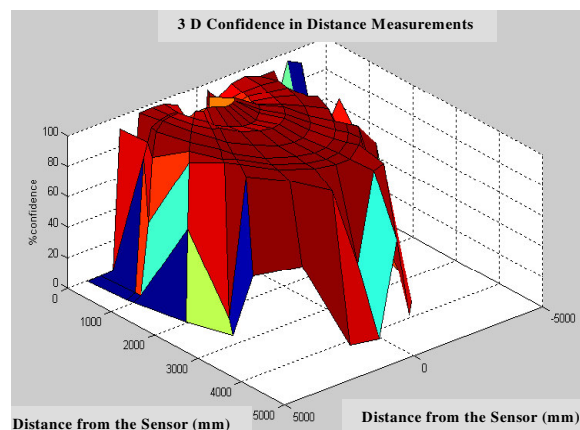Fig. 6. Measurements and Errors with Target Distance and Azimuth.

Fig. 7. Confidence in Distance Measurements as a function of the target's distance (from 0.221m to 4.221m) and azimuth relative to the sensor.

As seen in Figure 7, the confidence in distance measurements, for targets within a distance range of 0.221m to 3.221m and within an azimuth range of 27.9° to 150.3°, ranges from 92% to 100%. Outside of these azimuth angles, the confidence is only greater than 94% when the distance from the origin of the sensor is less than 2.721m and greater than 0.721m. It is worth noting the interesting fluctuation shown in Figure 7 where the % confidence between 0.2 and 0.9m is approximately 96%, but then decreases to about 93% between 0.9m and 1.2m, and finally rises again after 1.2m to 99% at around 1.8m; this may be due to the modulation of the light source.

D. Effect of Target Size

The size of the target directly affects the range at which it can be detected since the energy reflected from the target's surface is proportional to the target's surface area. Figure 8 shows the histograms of the measurements performed on 300mmx300mm, 200mmx200mm, and 100mmx100mm targets.
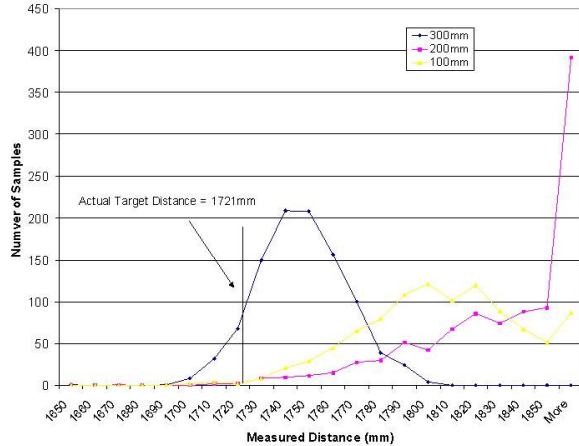

Fig. 8. Effect of Target size: Histograms of Distance Measurements of 3 target sizes at a fixed distance of 1.721m from the sensor's origin.

The distribution of histogram for the measurements performed on the 300mmx300mm target is narrower and centered closer to the true distance of the target than the histograms for the 200mmx200mm and 100mm x 100mm targets; thus indicating that distance measurements on targets smaller than 300mmx300mm will be error prone.

E. Effect of Target Color and Surface Properties

To test the effects of the reflective properties of various surfaces on the PBS-03JN infrared sensor, 13 targets were created with four different surface types. These surface types included matte colored cardboards (blue, yellow, red, black, and white), colored velvets (blue, red, black, and white), shiny cardboards (gold and silver), a mirror and an RGB127 target. The targets were tested at 1.231m, 1.721m and 2.231m, i.e. the middle of the manufacturer's guaranteed detection range. 1000 samples were taken for each target at the given distances and the distributions were analyzed to determine the effect of surface properties. The distribution of the histograms of measurements for the shiny targets is broad and inconsistent, as can be seen in Figure 9. The difference between the mean of the measurements and

the actual target distance for the shiny targets exceeds 162mm. The greater the reflectivity of the target (in order mirror, then silver, then gold), the higher the error and the broader the distribution becomes. Also, the farther the target from the sensor, the greater the standard deviation and the broader the distribution of readings due to reduced intensity of the reflected light from a target [5]. The maximum standard deviations of the distance measurements for the gold, silver, and mirror targets were σ_{max}=1873.94, σ_{max}=12032.56, and σ_{max}=29618.47 respectively (see Table II).
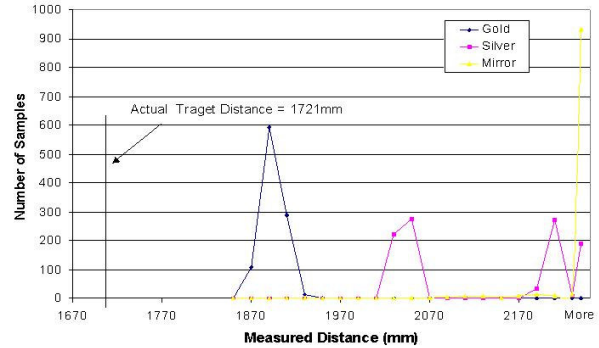

Fig. 9. Histogram of Distance Measurements from Shiny Targets (at a fixed distance of 1721mm from the sensor's origin).

The distribution of all the matte colored cardboard and velvet targets produced close Gaussian distributions centered at about 1.747m, as seen in Figure 10. The means of distance measurements for all the colors, including velvet cloth covered and the RGB 127 target, are similar, meaning that target's color or material does not affect the reading. The one exception is black velvet, which the sensor failed to detect; from the author's experience, the SICK LMS-200 laser scanner had a similar problem with black velvet targets but this was not formally characterized in [5].
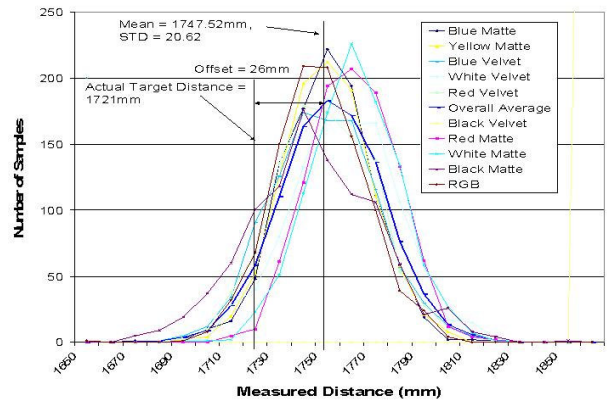

Fig. 10. Histogram of Distance Measurements form Colored Matte and Velvet Colth Covered Cardboard Targets (at a fixed distance of 1721mm from the sensor's origin).

The maximum standard deviation at 1,721mm was 26.72 for the black matte color with all other targets having a standard deviation of 10, see Table II. The standard deviations increase as the distance from the sensor increases but the % error remains within the same limits. In summary, the surface and color properties have no significant effects

on the mean or distribution of the readings taken by the sensor. The only exceptions are the shiny surfaces and the black velvet, which give erroneously high distance readings altogether (the maximum range).

TABLE II
CHANGE OF MEAN DISTANCE MEASUREMENT, STANDARD DEVIATION, AND PERCENT ERROR WITH TARGET SURFACE PROPERTIES AT 1.231M, 1.721M, AND 2.231M

	1231mm			1721mm			2231mm		
	Mean	StDev.	% Error	Mean	StDev.	% Error	Mean	StDev.	% Error
Blue	1347.7	11.70	9.49	1745.3	18.22	1.41	2255	34.35	1.08
Red	1354.2	10.85	10.01	1755.9	17.43	2.03	2236	34.19	0.23
Yellow	1346.8	10.14	9.41	1745.3	18.13	1.42	2244.3	33.22	0.60
White	1319.7	11.72	7.21	1756.5	18.42	2.06	2261.8	37.67	1.38
Black	1285.1	15.20	4.39	1739.9	26.72	1.10	2286.8	54.31	2.51
127 RGB	1324.2	11.52	7.57	1742.4	18.68	1.24	2232.1	35.59	0.05
Blue Velvet	1305.5	14.05	6.05	1744	21.50	1.34	2292	46.36	2.73
Red Velvet	1312	12.88	6.58	1744.6	20.93	1.38	2289.9	46.79	2.64
White Velvet	1322.6	13.40	7.44	1752.2	21.72	1.82	2281.4	46.11	2.26
Black Velvet	61608	18.27	4904.7	61610.8	17.48	3479.9	61618	14.86	2661.9
Gold	1446.3	79.70	17.49	1883.6	12.41	9.44	2544.1	1873.94	14.04
Silver	1996	4166.1	62.14	7923.3	12032.5	360.18	2663.6	108.22	19.39
Mirror	1350.3	16.2	-21.53	6424.8	14899.6	273.16	31623	29618.4	1317.4

F. Effect of Incidence at the Target

When the target is not perpendicular to the detection beam, the true distance between the range-finder and the target is harder to determine. As illustrated in Figure 11, if there is a distance offset between the range-finder's measurement origin and the center of the target, q or p not equal to 0, there an additional error in the distance measurement, $e = \pm(p+b)\tan\theta$ (5), to be accounted for when is θ different from $\tilde{0}$. This error can be eliminated by taking a pair of measurements at $\pm\theta$ for every distance and averaging them. If there is no offset, $p=q=0$, then the distance from the sensor to the target remains _ab_ regardless of the target's orientation, i.e. regardless of the beam's incidence angle to target [5]. The change in the effective surface area of the target, due to change of target angle, and specular reflections are other potential sources of error.
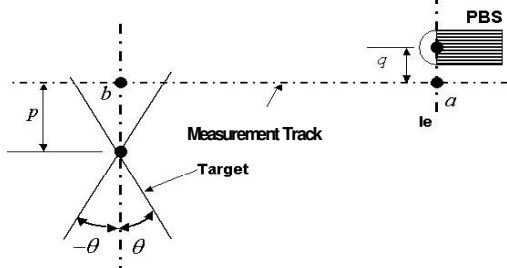

Fig. 11. Error Introduced by Incidence Angle and offset Distance between Target and the Sensor's Origin (adapted from [5]).

To test the effect of the incidence angle, the RGB 127 target was placed 2031mm from the origin of the sensor. Using a protractor the target's angle θ was adjusted from –70° to +70° in increments of 10° with 1000 data points

acquired at each angle. The data pairs were averaged so that the data represents 0°, ±10°, ±20°, ±30°, ±40°, ±50°, ±60°, and ±70°. Figure 12 shows the distribution of the measured data at these angles relative to each other.
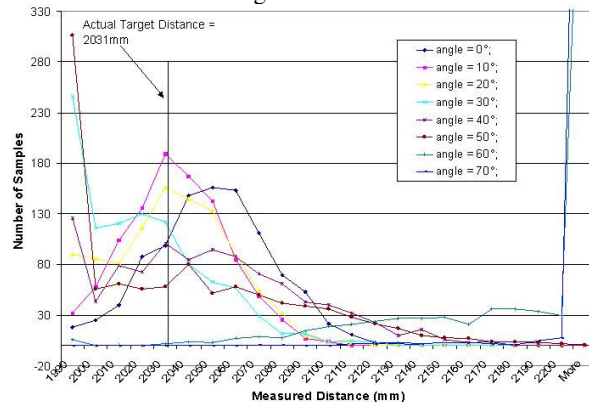

Fig. 12. Distribution of Measured Distances at Different Target Angles.

It is clear from the figure that the histograms peak around 2031mm with a rather broad distribution for all target angle pairs. The curves of 0°, ±10°, and ± 20° have the most similar distribution with a mean closest to the true target distance of 2031mm. Angles ±40° and ±50° have lower peaks and broader distribution but have a mean close to the true target distance and low % error, as can be seen in Table III. These angles should not cause significant error in measurement data as the % error is less than 0.7%. A target angle of ±30° has a lower mean of 2012.9mm and does not peak as the other angles do but instead has a downward sloping trend. Despite this trend, the % error is still less than 1%. All angles greater than 50° have a broader distribution of measured data and a great increase in the mean value of measurements (resulting in a low % error, making these angles inaccurate).

TABLE III
CHANGE OF MEAN DISTANCE MEASUREMENT, STANDARD DEVIATION, AND PERCENT ERROR WITH DIFFERENT INCIDENT ANGLES

	Mean	StDev.	% Error
angle = 0°	2045.57	25.90	0.67
angle = 10°	2029.74	21.77	0.11
angle = 20°	2027.32	26.93	0.23
angle = 30°	2012.19	31.91	0.98
angle = 40°	2039.81	44.96	0.38
angle = 50°	2025.23	58.66	0.33
angle = 60°	12033.58	13957.09	492.20
angle = 70°	26064.38	11955.99	1182.69

G. Characterization of The Mixed Pixel Problem

Due to the divergence of the scanning beam, when the beam of the infrared sensor is at the edge of a target, it hits both the foreground and background and returns a distance reading somewhere in between the distances of the foreground and the background [5]. To test the effect of mixed pixels the white matte target was placed 1600mm from the sensor's origin and a white matte background was placed 2m from the sensor's origin. From this distance 5

scan beams hit the target, beams 59 through 63, and the rest hit the background. The 2 beams on either side of the 5 that struck the target hit the edge of the target giving the "mixed pixel" result. The results of the 1000 averaged scans can be seen in Figure 13.
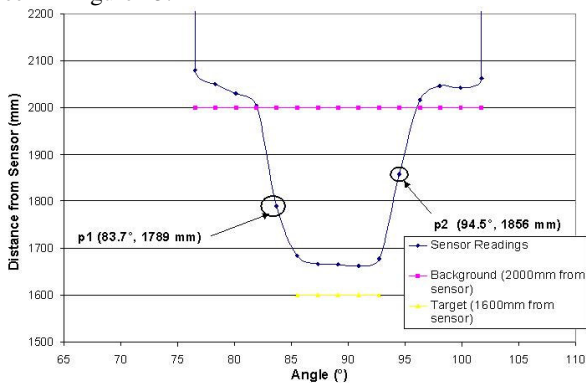

Fig. 13. Mixed Pixel Problem.

The results of the mixed pixel phenomenon are not a result of averaging multiple scans and can be seen in a single scan. A similar phenomenon can be observed when there is a sudden change in reflectivity of a surface [5].

H. Comparison of PBS-03JN Infrared Sensor to SICK LMS-200 Laser Scanner

The operation of HOKUYO PBS-03JN infrared sensor is similar to that of the SICK LMS-200 laser scanner. Table IV illustrates the difference in specifications of the two sensors. Compared to the LMS-200, the PBS-03JN sensor is smaller, lighter in weight, cheaper, consumes less power, and has a good angular resolution. However, the infrared sensor has a shorter range (up to 3 meters- adequate for many applications including indoor mapping and obstacle avoidance on slower mobile platforms), and larger measurement errors (in the range of 10.5 cm, comparable to that of the Polaroid ultrasonic range finders [2]). Advantages of the SICK LMS-200 laser scanner include much greater detection range, greater accuracy, higher angular resolution, and an adjustable resolution angle. In addition, the laser scanner has a faster response time than the PBS-03JN sensor in terms of activating the digital outputs when an obstacle is detected inside a pre-defined protected region; however, this does not have a direct impact on 2-D mapping applications.

TABLE IV
SPECIFICATIONS OF PBS-03JN INFRARED SENSOR AND LMS-200

Items	PBS-03JN	LMS-200
Size	75x70x60mm	155x210x156mm
Total Weight	500g	4500g
Angular Resolution	1.8°	1°/ 0.5°/ 0.25°
Response Time	180msec or less	13/ 26/ 53 ms
Angular Scanning Range	217.8° (178.2° usable)	180°
Range	0.2m to 3m	80m
Interface Method	RS-232C	RS422/ RS232
Power Source/ Consumption	24VDC (18 to 30 VDC, 10% ripple) @ 250mA	24VDC ± 15% @750mA
Warm-up Time	1hr19min	3hrs
Absolute Max. Error	105mm	17 mm
Approximate Cost	$1,000	$4,000

V. CONCLUSION

The infrared range finder PBS-03JN is a cost effective alternative to the laser range-finders in indoor environments where the required obstacle detection range does not exceed 3m, and where measurement errors in order of 10 cm are tolerable. The sensor is attractive for battery-powered applications, due to significantly lower power consumption, and/or hand-propelled mobile platforms, due to its lightweight. This range finder is an appropriate perception system for robotic walkers and other assistive devices, such as our intended application (see [11, 12, and 13]). Both sensors are ineffective at sensing materials with high reflectance, such as gold and silver surfaces, as well as black velvet/ cloth materials.

REFERENCES

[1] Jose Jimenez, Jesus Urena, Manuel Mazo, Alvaro Hernandez, Enrique Santso, "Three-Dimensional Discrimination Between Planes, Corners and Edges Using Ultrasonic Sensors", Proc. ETFA/IEEE Conf., Vol. 2, pp. 692-699, Sept. 2003.
[2] Data sheets for the Polaroid Ultrasonic Range-Finders, Polaroid Corporation.
[3] Teruko YATA, Akihisa OHYA, Shin'ichi YUTA, "A fast and accurate Sonar-ring Sensor for a Mobile Robot", Proc. Of IEEE Int. Conf. on Robotics and Automation, Detroit, Michigan, May, pp.630-636, 1999.
[4] H. Zreak, M. Alwan, M. Khaddour. "A Fuzzy Approach to Map Building", Lecture Notes in Artificial Intelligence 1611 "Multiple Approaches to Intelligent Systems", Proceedings of the 12th International Conference on Industrial and Engineering Applications of Artificial Intelligence and Expert Systems, IEA/AIE-99, Springer-Verlag, Cairo, Egypt, May/June 1999, pp. 33-42.
[5] Cang Ye, Johann Borenstein, "Characterization of a 2-D Laser Scanner for Mobile Robot Obstacle Negotiation", Proc. IEEE Int. Conf. On Robotics and Automation, Washington, DC, December, pp. 2512-2518, 2002.
[6] Terawaki, "Measuring Distance Type Obstacle Detection Sensor PBS-03JN Instruction Manual", Hokuyo Automatic Co., LTD., April 2004, pp. 1-19.
[7] http://www.sick.de/de/products/categories/auto/lasermeasurementsystemsindoor/lms200indoor/en.html
[8] Heo-Hui Kim, Yun-Su Ha, Gang-Gyoo Jin, "A Study of the Environmental Map Building for a Mobile Robot Using Infrared Range-finder Sensors", Proc. IEEE Intl. Conf. On Intelligent Robots and Systems, Las Vegas, NV, October, pp. 711-716, 2003.
[9] Yukio Nagira, "Measuring Distance Type Obstacle Detection Sensor PBS Series: Communication Protocol between PBS and PC", Hokuyo Automatic Co., LTD., July 2002, pp. 1-3.
[10] C. Ye, J. Borenstein, "A Novel Filter for Terrain Mapping with Laser Rangefinders", IEEE Trans on Robotics, Vol. 20, No. 5, pp. 913-921 Oct.2004.
[11] Wasson, G., Gunderson, J., Graves, S., Felder, R. "An Assistive Robotic Agent for Pedestrian Mobility", 2001 International Conference on Autonomous Agents: 169-173.
[12] Wasson, G., Sheth, P., Alwan, M., Huang, C. Ledoux, A. "User Intent in a Shared Control Framework for Pedestrian Mobility Aids", 2003 IEEE Intl. Conf. on Intelligent Robots and Systems (IROS '03).
[13] G. Wasson, P. Sheth, A. Ledoux, C. Huang, M. Alwan. "A Physics-Based Model for Predicting User Intent in Shared-Control Pedestrian Mobility Aids", In Proc of the 2004 IEEE/RSJ International Conference on Robots and Systems, Sendai, Japan, October 2004.